The micro-mechanisms of failure
of nodular cast iron

Alan Vaško[1], Mária Chalupová[2]

[1]Ing. PhD., University of Žilina, Faculty of Mechanical Engineering, Department of Materials Engineering, e-mail: alan.vasko@fstroj.uniza.sk
[2]Ing., University of Žilina, Faculty of Mechanical Engineering, Department of Materials Engineering

Abstract The contribution deals with a comparison of the micro-mechanisms of failure of nodular cast irons at static, impact and fatigue stress. Several specimens of ferrite-pearlitic nodular cast irons with different content of ferrite in a matrix were used for metallographic analysis, mechanical tests and micro-fractographic analysis. Mechanical properties were found by static tensile test, impact bending test and fatigue tests. The micro-fractographic analysis was made with use of scanning electron microscope VEGA II LMU on fracture surfaces of the specimens fractured by these mechanical and fatigue tests. Fracture surfaces of analysed specimens are characteristic of mixed mode of fracture. Micro-mechanism of failure of nodular cast irons is dependent on the method of stress.

Key words nodular cast iron, ferrite-pearlitic matrix, mechanical properties, micromechanisms of failure

1. Introduction

Nodular cast iron is widely used for the production of cast engineering components when high strength, plasticity and impact resistance are required, such as crankshafts, connecting rods and pistons. The wear resistance of nodular cast iron is comparable with some of the best grades of steel and superior to grey cast iron and moreover, provides the advantages of design flexibility and low cost of casting process (KONEČNÁ R. 2006).

The mechanical properties and micro-mechanisms of failure of nodular cast iron depend on many technological factors, such as charge composition, chemical composition, inoculation and modification method and additives, wall thickness of cast, cooling rate and many others and consequently on microstructure (especially shape, size and count of graphite nodules, content of ferrite in the matrix). The matrix of nodular cast iron is composed of ferrite and pearlite; the ratio of which can vary from fully ferritic to fully pearlitic over the whole spectrum of their mixtures. Ferrite is typically a ductile phase characterized by low strength while pearlite is a brittle phase with high strength. Failure of ferritic/pearlitic nodular cast iron is the result of competing damage mechanisms (KONEČNÁ R. 2004).

The contribution deals with comparison of the mechanical properties and micro-mechanisms of failure of the specimens of nodular cast irons fractured by static tensile test, impact bending test and fatigue tests.

2. Experimental material and methods

Three specimens of nodular cast iron with different microstructure were used for experiments. Chemical

composition of the specimens is approximately identical (eutectic degree $S_c \approx 1.2$) but it was achieved by a different charge composition. Therefore their microstructure is different. The basic charge of individual melts was formed by A different ratio of pig iron and steel scrap. For the regulation of chemical composition the additive of carburizer and metallurgical silicon carbide SiC90 was added. For modification, the Fe-SiMg7 modifier was used and for inoculation the FeSi75 inoculant was used.

Experimental bars (diameter 32 mm and length 350 mm) were cast from all the melts and consequently experimental specimens for the static tensile test, impact bending test and fatigue tests were made (VAŠKO A. 2008).
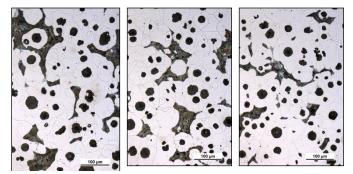
The metallographic analysis of the specimens was made by the light metallographic microscope Neophot 32. The specimens for metallographic analysis were taken out from the cast bars and prepared using the usual metallographic procedure. The microstructure of specimens was evaluated by STN EN ISO 945 (STN 42 0461) and by automatical image analysis using NIS Elements software (SKOČOVSKÝ P. 2007, BELAN J. 2013, HURTALOVÁ L. 2013.). The image analysis was used for the evaluation of count of graphitic nodules per unit area and the content of ferrite in the matrix.

The static tensile test was made by STN EN 10002-1 by means of the testing equipment ZDM 30 with a loading range F = 0 to 50 kN. The impact bending test was made by STN EN 10045-1 by means of the Charpy hammer PSW 300 with a nominal energy of 300 J (VAŠKO A. 2009). The fatigue tests were made by STN 42 0362 at high-frequency sinusoidal cyclic push-pull loading (frequency f ≈ 20 kHz, stress ratio R = −1, temperature T = 20 ± 5 °C) using ultrasonic testing equipment KAUP-ZU (BOKŮVKA O. 2002, VAŠKO M. 2013).

The micro-fractographic analysis was made by the scanning electron microscopes Tesla BS 343 and VEGA II LMU on fracture surfaces of the specimens fractured by static tensile test, impact bending test and fatigue tests.

3. Experimental results and discussion

From a microstructural point of view all the specimens are ferrite-pearlitic nodular cast irons with a different content of ferrite and pearlite in the matrix and a different size of graphite and count of graphitic nodules per mm^2 (Fig. 1). Different content of ferrite and pearlite in the matrix as well as different size of graphite and count of graphitic nodules in the individual specimens are caused by different charge composition.

a) specimen 1   a) specimen 3   a) specimen 5
Fig. 1. Microstructure of the specimens from experimental bars, etched 1% Nital.

Source: own study

The results of the evaluation of microstructure of the specimens by STN EN ISO 945 (STN 42 0461) and by image analysis (content of ferrite and count of graphitic nodules) are presented in Tab. 1.

The lowest content of ferrite (approximately 62 %) was found out in the specimen 1, the highest content of ferrite (78 %) is in the specimen 5. The size of graphite is from 30 to 120 μm, but in all the specimens the size within 30-60 μm predominates. The average count of graphitic nodules per unit area in the specimen 1 is lower than in the specimens 3 and 5 (almost 200 mm^{-2}).

The mechanical tests (i.e. static tensile test, impact bending test and fatigue tests) were realized on the specimens made from cast bars. The results of mechanical tests, that are tensile strength R_m, elongation A, absorbed energy K and fatigue strength σ_c, are given in Tab. 1.2.

The tensile strength, elongation and absorbed energy in the specimen 1 is lower than in the specimens 3 and 5.

Table 1.1. Evaluation of microstructure of the specimens

Specimen	microstructure by STN EN ISO 945 (STN 42 0461)	content of ferrite (%)	count of graphitic nodules (mm^{-2})
1	60%VI5/6+40%V6 – Fe80	61.6	104.3
3	80%VI6 + 20%V6 – Fe94	74.0	199.8
5	70%VI5/6+30%V6 – Fe94	78.0	179.8

Source: own study

Table 1.2. Mechanical properties of the specimens

Specimen	tensile strength R_m (MPa)	elongation A (%)	absorbed energy K (J)	fatigue strength σ_c (MPa)
1	500.8	1.3	6.4	
3	539.0	4.0	30.6	218
5	515.7	3.7	17.2	191

Source: own study

The mechanical properties are dependent on microstructure, especially on the character of matrix (content of ferrite and pearlite) and also on the size and count of graphitic nodules, which have a connection with the charge composition. The mechanical properties in the specimens of nodular cast iron with higher content of ferrite in the matrix and higher count of graphitic nodules are better than in the specimen with lower content of ferrite.
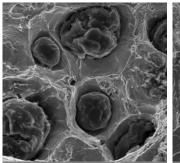
The micro-fractographic analysis was made by the scanning electron microscope Tesla BS 343 on fracture surfaces of specimens from experimental bars fractured by the static tensile test (Fig. 2) and the impact bending test (Fig. 3).
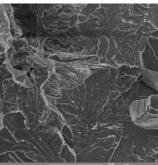
Fracture surfaces of the specimens fractured by the static tensile test are characteristic of a mixed mode of fracture. In the specimens of nodular cast iron with lower content of ferrite in the matrix, transcrystalline cleavage of ferrite with an inclination to intercrystalline cleavage of ferrite around graphitic nodules (Fig. 2a) was observed. In the specimens of nodular cast iron with higher content of ferrite in the matrix, transcrystalline cleavage of ferrite with river drawing on facets (Fig. 2b) and transcrystalline ductile failure of ferrite with dimple morphology (Fig. 2c) was observed. The ratio of transcrystalline ductile failure of

ferrite (at the expense of transcrystalline cleavage) is increased with increasing content of ferrite in the matrix. Pearlite was a failure especially due to transcrystalline continuous cleavage in all the specimens (Fig. 2d). In the specimens with a higher content of ferrite in the matrix, transcrystalline ductile failure of pearlite was also observed.

a) intercrystalline cleavage of ferrite

b) transcrystalline cleavage of ferrite
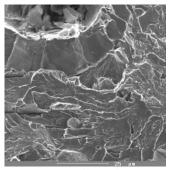
c) transcrystalline ductile failure of ferrite

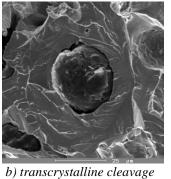d) transcrystalline continuous cleavage of pearlite

Fig. 1.2. Micromechanisms of failure of ferrite and pearlite at static stress, SEM.

Source: own study

Similarly, fracture surfaces of the specimens fractured by the impact bending test are characteristic of a mixed mode of fracture. In the specimens of nodular cast iron with lower content of ferrite in the matrix, intercrystalline cleavage of ferrite was observed around graphitic nodules (Fig. 3a) and transcrystalline cleavage of ferrite in the rest of area. In the specimens of nodular cast iron with higher content of ferrite in the matrix, transcrystalline cleavage of ferrite with river drawing on facets (Fig. 3b) and transcrystalline ductile failure of ferrite with dimple morphology (Fig. 3c) was observed. The ratio of transcrystalline ductile failure of ferrite (at the expense of transcrystalline cleavage) is

increased with increasing content of ferrite in the matrix. In all the specimens, transcrystalline continuous cleavage of pearlite as well as transcrystalline ductile failure of pearlite (Fig. 3d) was observed.
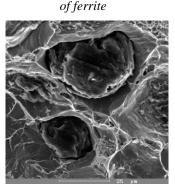
The results of micro-fractographic analysis correspond to the results of metallographic analysis and mechanical tests.

a) intercrystalline cleavage of ferrite

b) transcrystalline cleavage of ferrite

c) transcrystalline ductile failure of ferrite

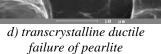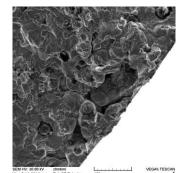*d) transcrystalline ductile failure of pearlite*

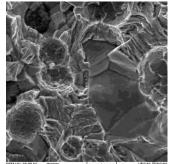*Fig. 3. Micromechanisms of failure of ferrite and pearlite at impact stress, SEM.*

Source: own study

The micro-fractographic analysis of the specimens from experimental bars fractured by fatigue tests was made by the scanning electron microscope VEGA II LMU (Fig. 4).

Fracture surfaces of the specimens after fatigue failure do not show any remarkable differences; they are characteristic of a mixed mode of fracture. The fatigue fracture was initiated by casting defect (Fig. 4a). The fatigue fracture is characteristic of intercrystalline fatigue failure of ferrite around graphitic nodules and transcrystalline fatigue failure of ferrite and pearlite in the rest of the area (Fig. 4b). The final rupture is characteristic of transcrystalline ductile failure of ferrite with dimple morphology (Fig. 4c) and tran-

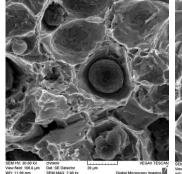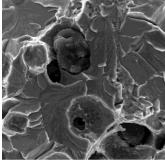scrystalline cleavage of ferrite and pearlite with river drawing on facets (Fig. 4d).

a) initiation of fatigue failure

b) transcrystalline and intercrystalline fatigue failure

c) final rupture – transcrystalline ductile failure

d) final rupture – transcrystalline cleavage

Fig. 4. Micromechanisms of failure of ferrite and pearlite at fatigue stress, $\sigma_a = 272$ MPa, $N_f = 1.1 \times 10^7$ cycles, SEM.

Source: own study

4. Conclusions

The mode of failure of structural components depends especially on the content of ferrite in the matrix and its purity, which has a connection with the charge composition. Failure of ferrite was due to intercrystalline cleavage over transcrystalline cleavage with river drawing on facets to transcrystalline ductile failure with dimple morphology. A higher ratio of transcrystalline ductile failure has a connection with higher content of ferrite in the matrix. Failure of pearlite was especially caused by transcrystalline continuous cleavage and in a few isolated cases, also by transcrystalline ductile failure.

The fatigue failure has a mixed character of fracture (intercrystalline and transcrystalline fatigue fail-

ure) in all the specimens; the intercrystalline fatigue failure predominates near graphitic nodules and the transcrystalline fatigue failure predominates in the rest of the area. No significant differences were observed by the comparison of fracture surfaces of the analysed specimens.

Acknowledgements

References

1. BELAN J. 2013. *Study of advanced Ni-base ŽS6K alloy by quantitative metallography methods*. „Manufacturing Technology". Vol. 13, No. 1, p. 2-7.

2. BOKŮVKA O., NICOLETTO G., KUNZ L., PALČEK P., CHALUPOVÁ M. 2002. *Low & high frequency fatigue testing.* EDIS. Žilina.

3. HURTALOVÁ L., TILLOVÁ E. 2013. *Elimination of the negative effect of Fe-rich intermetallic phases in secondary (recycled) aluminium cast alloy.* „Manufacturing Technology", Vol. 13, No. 1, p. 44-50.

4. KONEČNÁ R., BUJNOVÁ P., NICOLETTO G. 2004. *Failure mechanisms in ferritic-pearlitic nodular cast iron.* „Engineering Mechanics". Vol. 11, No. 5, p. 319-323.

5. KONEČNÁ R., LEJČEK P., NICOLETTO G., BARTUŠKA P. 2006. *Role of composition heterogeneity on fracture micromechanisms of nodular cast iron.* „Materials Science and Technology". Vol. 22, No. 12, p. 1415-1422.

6. SKOČOVSKÝ P., VAŠKO A. 2007. *Kvantitatívne hodnotenie štruktúry liatin.* EDIS. Žilina.

7. LESTYÁNSZKA ŠKŮRKOVÁ K. 2013. *Using the Shewhart control charts by process control.* Production Egineering Archives. Vol. 1(1), p.29-31.

8. VAŠKO A. 2008. *Influence of SiC additive on microstructure and mechanical properties of nodular cast iron.* „Materials Science (Medžiagotyra)", Vol. 14, No. 4, p. 311-314.

9. VAŠKO A., SKOČOVSKÝ P. 2009. *Vlastnosti a použitie materiálov.* EDIS. Žilina.

10. VAŠKO M., SÁGA M. 2013. *Application of fuzzy structural analysis for damage prediction considering uncertain S/N curve*. „Applied Mechanics and Materials", Vol. 420, p. 21-29.